

Field-scale application of a semi-analytical model for estimation of CO₂ and brine leakage along old wells

Michael A. Celia^{a,*}, Jan M. Nordbotten^{a,b}, Benjamin Court^a, Mark Dobossy^c, Stefan Bachu^d

^a Department of Civil and Environmental Engineering, Princeton University, Princeton, NJ, USA

^b Department of Mathematics, University of Bergen, Bergen, Norway

^c Geological Storage Consultants, Minneapolis, MN, USA

^d Alberta Innovates – Technology Futures, Edmonton, Alberta, Canada

ARTICLE INFO

Article history:

Received 2 January 2010

Received in revised form 13 October 2010

Accepted 14 October 2010

Available online 22 December 2010

Keywords:

Geological storage

Leakage

Semi-analytical solutions

Abandoned wells

Risk analysis

Site characterization

ABSTRACT

Carbon capture and geological storage (CCS) operations will require an environmental risk analysis to determine, among other things, the risk that injected CO₂ or displaced brine will leak from the injection formation into other parts of the subsurface or surface environments. Such an analysis requires site characterization including identification of potential leakage pathways. In North America, the century-long legacy of oil and gas exploration and production has left millions of oil and gas wells, many of which are co-located with otherwise good geological storage sites. Potential leakage along existing wells, coupled with layered stratigraphic sequences and highly uncertain parameters, makes quantitative analysis of leakage risk a significant computational challenge. However, new approaches to modeling CO₂ injection, migration, and leakage allow for realistic scenarios to be simulated within a probabilistic framework. Using a specific field site in Alberta, Canada, we perform a range of computational studies aimed at risk analysis with a focus on CO₂ and brine leakage along old wells. The specific calculations focus on the injection period, when risk of leakage is expected to be largest. Specifically, we simulate 50 years of injection of supercritical CO₂ and use a Monte Carlo framework to analyze the overall system behavior. The simulations involve injection, migration, and leakage over the 50-year time horizon for domains of several thousand square kilometers having multiple layers in the sedimentary succession and several thousand old wells within the domain. Because we can perform each simulation in a few minutes of computer time, we can run tens of thousands of simulations and analyze the outputs in a probabilistic framework. We use these kinds of simulations to demonstrate the importance of residual brine saturations, the range of current options to quantify leaky well properties, and the impact of depth of injection and how it relates to leakage risk.

© 2010 Published by Elsevier Ltd.

1. Introduction

Carbon capture and geological storage (CCS) has been identified by many recent studies as a critical technology for any realistic strategy to solve the carbon problem (IEA, 2004, 2008a,b; Pacala and Socolow, 2004; IPCC, 2005; MIT, 2007; McKinsey and Company, 2007; Sheppard and Socolow, 2007). Among the possible formations available for storage, deep saline aquifers have the largest capacity (IPCC, 2005) and are relatively ubiquitous. However, because of the enormous scale of the problem, any full-scale implementation of CCS will likely require use of other geological media such as oil and gas reservoirs and coal beds (IPCC, 2005).

When considering geological storage of CO₂, an important environmental concern is leakage of the injected CO₂, as well as possible leakage or large-scale displacement of the resident brine. One potentially important leakage pathway is associated with the century-long legacy of oil and gas exploration and production, which has resulted in many millions of wells having been drilled around the world through otherwise excellent caprock formations. Because a successful CO₂ storage operation requires a competent caprock formation overlying the injection formation, these oil and gas wells may compromise the success of storage operations by providing preferential flow pathways through the caprock. This is especially true in North America, where millions of oil and gas wells have been drilled since the late 1800s—see Fig. 1.

Gasda et al. (2004) analyzed the spatial density of wells that perforate a particular formation in the Alberta Basin in Canada. Their results indicated that tens to hundreds of wells might be contacted by a typical CO₂ plume. If the area of concern is expanded

* Corresponding author. Tel.: +1 609 258 5425; fax: +1 609 258 2760.
E-mail address: celia@princeton.edu (M.A. Celia).

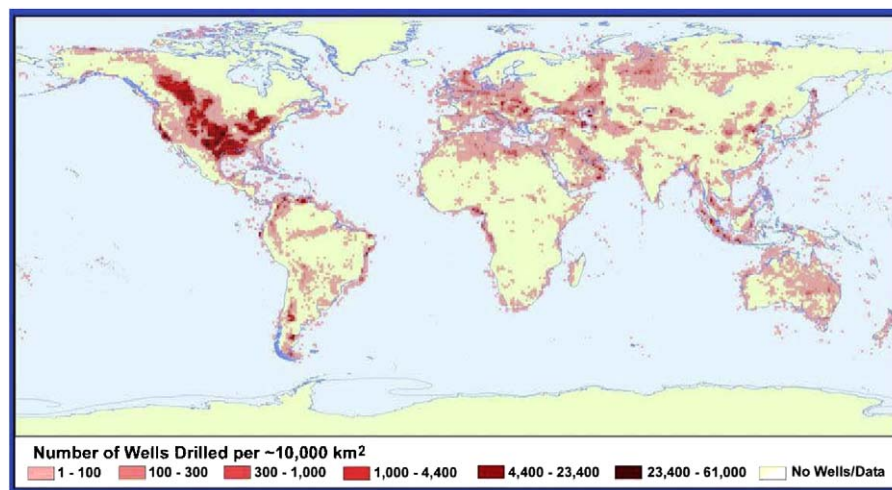


Fig. 1. Worldwide density of wells (from IPCC, 2005).

to include regions of possible brine migration and leakage, the number of wells of concern increases further. For a large-scale injection operation that continues over several decades, the domain that needs to be analyzed may be on the order of thousands of square kilometers. Within that domain, the vertical structure, particularly the major layers of permeable (aquifer) and essentially impermeable (caprock or aquitard) formations, must be taken into account (see, for example, Nordbotten et al., 2004). Within this three-dimensional domain, many hundreds of wells may exist, each with a different depth of penetration, and with properties that have large uncertainty. The uncertainty of the key parameters associated with well leakage, coupled with the underlying complexity associated with the physics and mathematics of two-phase flow (CO₂ and brine), make this a computationally challenging problem. Among others, Schnaar and Digiulio (2009) provide a useful review summarizing different modeling approaches and Michael et al. (2009a,b) provide a good overview of the current state of scientific knowledge on CO₂ storage in saline aquifers and experience from existing storage operations.

To overcome computational limitations of existing multi-phase simulators, a new set of computational models have been developed that can solve problems involving large spatial domains with many vertical layers and many existing wells. The basic components of the model can be found in Nordbotten et al. (2004, 2005a,b, 2009), Nordbotten and Celia (2006a,b), and Celia and Nordbotten (2009, 2010). Simple example applications of different parts of the model can be found in those papers as well as in Nordbotten et al. (2005a), Celia et al. (2006), Kavetski et al. (2006), and Bachu and Celia (2009). The model takes advantage of specific assumptions, consistent with the physics and chemistry of the system, to simplify the equations such that analytical and semi-analytical solutions can be obtained (see Celia and Nordbotten, 2009, 2010).

In the present work we demonstrate the application of this overall modeling approach for a specific field site in Alberta, Canada. The location corresponds to an area where four large power plants currently operate, emitting collectively about 30 million tonnes (Mt) of CO₂ per year (Michael et al., 2009c). We use detailed stratigraphic descriptions and actual locations and depths of 1146 wells over a study area of 2500 km². We use the model to demonstrate the most important characteristics of the problem, including the vertical structure in the stratigraphic sequence, the nature of possible leakage in such systems, the importance of injection location within the vertical sequence and the sensitivity of maximum injectivity on residual brine saturations. Model results show how leakage risk can change as a function of depth of injection due to a number of

competing factors. The results also illustrate the potentially limiting nature of injectivity in deep sedimentary basins like the Alberta Basin, where the existence of large capacity does not guarantee that a site is appropriate, because the rate at which the overall capacity can be accessed must be considered. As such, injectivity can be more important than capacity. Our model calculates both CO₂ and brine migration and leakage throughout the duration of the active period of CO₂ injection.

The paper is organized as follows. We begin with an overview of the model used in the analysis. Next we describe the field site, including the different permeable formations and their properties, the location and depth of all known oil and gas wells in the area, and the choice of domain and associated boundary conditions. Next we present the simulations we have run, and focus our results on the issues of (1) critical well properties, (2) the trade-off between depth of injection and risk of leakage, (3) the important role of injectivity limitations, and (4) comparison between CO₂ and brine leakage characteristics. We conclude with comments about modeling options and the kinds of analysis tools that are needed to further refine the calculations presented herein.

2. Computational model

The computational model used in this work is based on a set of analytical and semi-analytical solutions for CO₂ injection (Nordbotten and Celia, 2006a), leakage along segments of wells (Nordbotten et al., 2009), and upconing in the vicinity of leaky wells (Nordbotten and Celia, 2006b). These individual components are integrated into an overall solution algorithm that can accommodate arbitrary numbers of sedimentary layers (aquifers and aquitards) and arbitrary numbers of potentially leaky wells. The combined algorithm is described in Nordbotten et al. (2009) and Celia and Nordbotten (2009). These algorithms and calculations complement the related recent work of Grimstad et al. (2009), Pawar et al. (2009), and Stauffer et al. (2009), among others, who have studied different aspects of CO₂ injection and leakage.

2.1. CO₂ plume evolution

The fundamental building block of the model is a solution for a single injection well in a horizontal, confined, homogeneous deep saline aquifer. The model uses the assumption of strong buoyant segregation, driven by the large density difference between the CO₂ and brine, coupled with the complementary assumption that once the fluids are separated by buoyancy, they attain

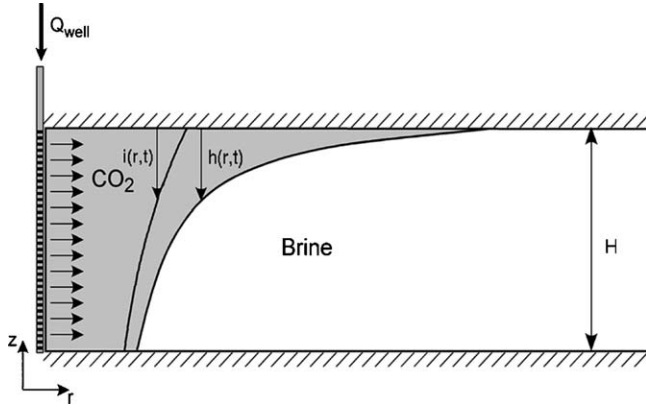


Fig. 2. Schematic of CO₂ plume of thickness $h(r, t)$. Also shown is the drying front, with dry CO₂ having thickness $i(r, t)$ (from Nordbotten and Celia, 2006a).

vertical equilibrium in their pressure distributions. Those equilibrium pressure profiles couple with the local capillary pressure function to give a vertical profile of the fluid saturations. If the capillary transition zone associated with the local capillary pressure is small relative to the thickness of the formation, then the transition zone can be approximated by a sharp interface, thereby providing a simpler vertical representation of the saturation profile. For the present model, we assume vertical equilibrium coupled with a sharp interface. Using these assumptions, coupled with the assumption of homogeneity of material properties within a given formation and horizontal top and bottom boundaries for the formation, Nordbotten and Celia (2006a) derived a similarity solution for the system shown in Fig. 2. The solution involves an interface separating the leading edge of the CO₂ and the resident brine, with the thickness of the CO₂ plume denoted by $h(r, t)$, where r is radial distance from the injection well and t is time since start of injection. Behind this front is a region of CO₂ and brine, where the brine is assumed to be at residual saturation. If dry CO₂ is injected into the formation, the water in the residual brine saturation will eventually evaporate and disappear, leading to the formation of a drying front, behind which only dry CO₂ exists in the pore space. The drying front is denoted by $i(r, t)$ in Fig. 2. The solutions of Nordbotten and Celia (2006a) solve the system for the location of the two fronts, $h(r, t)$ and $i(r, t)$, as well as the pressure in the formation, taken as the pressure along the bottom, $p_{bot}(r, t)$. Knowledge of p_{bot} and $h(r, t)$, coupled with the assumption of vertical equilibrium, allows the pressure to be determined at all points in the domain. The resulting set of nonlinear, coupled partial differential equations can be rewritten in terms of a similarity variable, χ , such that the three unknowns are a function of only χ , and the partial differential equations reduce to a set of ordinary differential equations. The variable χ is defined by

$$\chi = \frac{2\pi H \phi (1 - S_B^{res}) r^2}{Q_{well} t} \quad (1)$$

where H is the thickness of the aquifer, ϕ is the porosity of the injection formation, S_B^{res} is the residual saturation of the brine, and Q_{well} is the volumetric injection rate of CO₂. Note that χ is dimensionless, and is proportional to r^2/t . Note also that the boundary condition applied at the well is a constant flux given by Q_{well} . The resulting ordinary differential equations only need to be solved once, resulting in the solutions $h(\chi)$, $i(\chi)$, and $p_{bot}(\chi)$. Then, for any values of space (r) and time (t), a value of χ is determined and the solutions for the interface locations and pressure can be solved immediately. In the following, we will not consider the drying front, and will only concentrate on the invading CO₂ front $h(r, t)$ and the pressure field $p_{bot}(r, t)$.

While these ordinary differential equations are useful in that they provide relatively simple solutions for both the pressure field and the CO₂ plume, the solutions simplify further depending on the dimensionless grouping Γ , given by

$$\Gamma = \frac{2\pi(\rho_B - \rho_C)gkH^2}{\mu_B Q_{well}} \quad (2)$$

where ρ_B and ρ_C denote density for brine (B) and CO₂ (C), respectively, g is the gravitational acceleration, k is permeability of the formation, and μ_B is the viscosity of the brine. This dimensionless group, defined elsewhere as the gravitational number (see, e.g., Kopp et al., 2009) represents the ratio of buoyancy forces to viscosity forces acting on the buoyant CO₂ and plays an important role in CO₂ storage capacity (Kopp et al., 2009). When values of Γ are small (for this work we use the cutoff value $\Gamma < 0.1$), the solutions for the CO₂ plume and the pressure field simplify further. In this simplified case, the expression for the CO₂ plume may be written as

$$h'(\chi) = \frac{h(\chi)}{H} = \frac{1}{\lambda - 1} \left(\sqrt{\frac{2\lambda}{\chi}} - 1 \right) \quad (3)$$

In this equation, the plume thickness is zero whenever the expression on the right side of Eq. (3) is negative, and is equal to H whenever the right side of the equation exceeds unity. The associated pressure field may be expressed as follows:

$$\Delta p'(\chi) - F(h') = \begin{cases} 0, & \chi \geq \Psi \\ -\frac{1}{2\Gamma} \ln\left(\frac{\chi}{\Psi}\right) + \Delta p'(\Psi), & \Psi > \chi > 2\lambda \\ \frac{1}{\Gamma} - \frac{\sqrt{\chi}}{\Gamma\sqrt{2\lambda}} + \Delta p'(2\lambda), & 2\lambda > \chi > \frac{2}{\lambda} \\ -\frac{1}{2\lambda\Gamma} \ln\left(\frac{\chi\lambda}{2}\right) + \Delta p'\left(\frac{2}{\lambda}\right), & \frac{2}{\lambda} > \chi \end{cases} \quad (4)$$

In these equations, λ is the mobility ratio, $\lambda = \lambda_C/\lambda_B$, which is the ratio of the phase mobilities $\lambda_C = k_{rel,C}/\mu_C$ and $\lambda_B = k_{rel,B}/\mu_B$, where $k_{rel,C}$ is the relative permeability of the rock to the CO₂ phase and $k_{rel,B}$ is the relative permeability to brine. In regions where $h > 0$, $k_{rel,C}$ is evaluated with the brine phase at residual saturation, which means the relative permeability will be less than one whenever the brine residual saturation is greater than zero. Because we focus only on injection scenarios in this work, the brine saturation is always equal to one ahead of the CO₂ front (that is, ahead of (or below) the interface $h(r, t)$), and therefore the value of $k_{rel,B}$ is always equal to one. In Eq. (4), p' is a dimensionless pressure, $\Delta p'$ denotes the change in pressure relative to the initial value, Ψ is the location of the outer boundary at which the pressure has not changed relative to the initial pressure, which is taken as being hydrostatic everywhere, and F is an offset term associated with the vertical pressure distribution. The three variables introduced above have the following definitions (see Nordbotten and Celia, 2006a and Nordbotten et al., 2009 for more details):

$$\Delta p' = \frac{p - p_0}{(\rho_B - \rho_C)gH} \quad (5a)$$

$$\Psi = \frac{4.5\pi H \phi k (1 - S_B^{res})}{\mu_B c_{eff} Q_{well}} \quad (5b)$$

$$F(h') = -\frac{\lambda}{\lambda - 1} \left[h'(\chi) + \frac{\ln[(\lambda - 1)h' + 1]}{\lambda - 1} \right] \quad (5c)$$

where p_0 is the initial pressure, and c_{eff} is the effective compressibility coefficient for the fluid and the solid matrix. We take the compressibility to be fixed and equal to the compressibility of brine, since most of the computational domain is filled with brine. We also comment that the definition of Ψ is based on the logarithmic

approximation to the exponential integral, and note that more specific treatment of pressure thresholds associated with the area of review estimation can be used in place of this specific expression for Ψ .

As stated previously, we ignore the drying front and the associated dry CO₂ region. Recent work (Pruess, 2009; Pruess and Muller, 2009) suggests that salt precipitation in the dry region may be significant—our use of residual brine saturation throughout the entire CO₂ region may be seen as using residual brine saturation to represent the fractional pore space occupied by either brine or precipitated salt. The solution in Eqs. (4) and (5) also ignores any diffuse leakage across the caprock formations. While contributing little to vertical mass transport, such diffuse leakage could have significant impact on the pressure fields, affecting Eqs. (4) and (5) including the location of the outer boundary of the pressure pulse, which is given by Eq. (5b). The recent work of Mathias et al. (2009a), Dentz and Tartakovsky (2009), Szulczewski and Juanes (2009), and Hesse et al. (2007, 2008) uses similar mathematical methods to study the CO₂ injection and migration problem, although none of these authors deals with leakage for the kinds of problems we consider herein. The recent work of Birkholzer et al. (2009), Zhou et al. (2008), Mathias et al. (2009b), and the older work of Hunt (1985), examines pressure propagation due to injection and the impacts of diffuse leakage.

These analytical solutions form one of the basic building blocks for the overall analysis of CO₂ plume and pressure evolution with leakage along wells in multi-layer, multi-well problems. They also form simple and powerful stand-alone tools to analyze the basic behavior of a plume of CO₂ and the associated pressure field in an aquifer into which CO₂ is injected, without adding the complications of wells and leakage. Eq. (3) provides a simple estimate for the plume size and thickness, and can easily give estimates for the location of the outer edge of a plume: set Eq. (3) to zero and find $\chi = 2\lambda$, which represents the outer edge of the plume, called $r_{\text{outerPlume}}$, located at

$$r_{\text{outerPlume}} = \sqrt{\frac{\lambda Q_{\text{well}} t}{\pi(1 - S_B^{\text{res}})\phi H}} \quad (6a)$$

Note that the outer edge of the CO₂ plume grows with the square root of time. Similarly, Eq. (5b) provides information about the maximum spatial extent of the pressure pulse and is obtained by imposing the following maximum pressure pulse outer radius in the brine region:

$$r_{\text{outer Pressure}} = \sqrt{\frac{2.25 kt}{\mu_b c_{\text{eff}}}} \quad (6b)$$

This follows from Nordbotten et al. (2004). Both of these equations are very useful for simple screening calculations, although we note that Eq. (6b) does not include the effects of diffuse leakage through the caprock.

2.2. Leakage along wells

Leakage along wells is treated as Darcy flow, using the two-phase extension of Darcy's Law. While we recognize the complicated flow paths that can be associated with leakage along wellbores, especially at small spatial scales, we focus our modeling on mathematical descriptions across relatively large distances along a well. In addition, we assume that in the majority of cases leakage will take place outside the well casing, along the complex zone that involves cement and residual drilling fluids in the annular space, as well as possible damaged rock zones caused by the drilling process (leakage that takes place through the well tubing is akin to a well blow out and needs to be dealt with differently). We lump all of these materials, and the complex flow paths through them, into

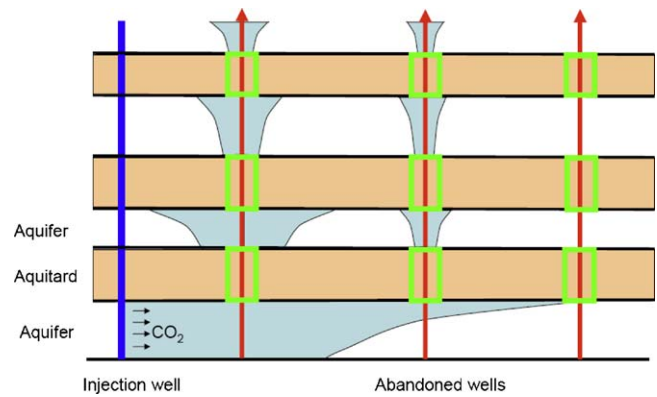


Fig. 3. Schematic of flow and leakage in a multilayer system. Well permeabilities are assigned to each segment of each well, as indicated by the boxes (modified from Kavetski et al., 2006).

a bulk 'effective' permeability coefficient that represents the ability of fluid to flow along a well. The permeability is meant to apply, in bulk, over a length along the well that corresponds to the thickness of a caprock formation. With reference to the schematic of flow and leakage given in Fig. 3, each potential leaky well will be characterized by an effective permeability assigned to each segment of the well that crosses an individual caprock formation. That is, if a well crosses some number, say N_c , of caprock formations, then it will be characterized by N_c different permeability values. How these values relate to one another, and perhaps to values in other wells, is discussed later in the paper.

With this idea in mind, the one-dimensional multi-phase version of Darcy's Law may be written to represent flow along a leaky well as follows:

$$q_\alpha = -\frac{kk_{\text{rel},\alpha}}{\mu_\alpha} \left(\frac{\partial p_\alpha}{\partial z} + \rho_\alpha g \right) \quad (7)$$

In this equation, q_α is the volumetric flux of phase α ($\alpha = B, C$) along the well (volume of phase α per area per time), assumed positive upward, and $k_{\text{rel},\alpha}$ is the relative permeability (dimensionless), taken to be a function of phase saturation, S_α , along the well. In this work, we have taken relative permeability to be a linear function of saturation along the well segment. We reiterate that the permeability, k , is interpreted as the effective permeability over the length of the caprock. Given that the length scale is set by the caprock thickness, we may write a discrete version of the Darcy equation with respect to the caprock segment as follows:

$$q_{\alpha,i} = -\frac{k_i k_{\text{rel},\alpha,i}}{\mu_\alpha} \left[\frac{p_{\alpha,i+} - p_{\alpha,i-}}{\ell_i} + \rho_\alpha g \right] \quad (8)$$

where subscript i denotes the i th caprock in the vertical sequence, and $i+$ and $i-$ denote values at the top and bottom of the caprock formation, respectively. We also assume this leakage flux occurs over an effective flow area A_{well} , such that $q_\alpha A_{\text{well}}$ gives the total volumetric flow rate along the well.

2.3. Interface upconing

The third important part of the simulation package we have developed is a solution that describes the so-called upconing of the CO₂–brine interface around a leaky well. The idea is that when a well is leaking, the flow of fluid along the well represents a net loss of mass in the formation from which the leakage is occurring (for example, the injection formation). This causes a local decrease in pressure around the well, which induces the CO₂–brine interface to move upward, reducing the thickness of the CO₂ plume in the vicinity of the leaky well. If the thickness goes to zero locally

at the well, then both brine and CO₂ can flow along the well. If the thickness of the plume remains greater than zero, then only CO₂ will flow along the well. And if the CO₂ plume has not yet reached the well, then only brine can leak along the well.

Our approach is to use an improved analytical solution to the interface upconing problem, as derived in Nordbotten and Celia (2006b). The solution uses existing interface thickness, pressure, and leakage conditions to determine the thickness of the CO₂ plume at a leaky well. If the thickness goes to zero, then an additional calculation is performed to determine the fraction of flow along the well that comes from each of the two fluids, CO₂ and brine. This is then used in the remainder of the calculations for the overall pressure and CO₂ fields.

2.4. Overall computational algorithm

The three major computational components, described in Sections 2.1, 2.2, and 2.3, form the core of our model. Details about how these are put together, the way discrete time-stepping is imposed, and other considerations are described in associated references by the authors (e.g., Nordbotten et al., 2009). We note that, contrary to traditional numerical models for these kinds of problems, our model has no spatial grid but rather uses analytical solutions in space that are associated with the physical features of the problem, specifically the wells and the permeable layers. However, because of the nonlinearity of the underlying equations, discrete time steps are required. Because of the discretization in time, we refer to the overall solution process as a semi-analytical algorithm.

The overall algorithm proceeds as follows. For any given time step, we begin by solving for pressures at each well segment in each permeable formation. This is based on superposition of solutions associated with individual wells, with coupling across formations due to the Darcy flows along leaky wells. The result of this step is a set of algebraic equations with the number of unknowns equal to the product of the number of wells times the number of permeable layers. Solution of this set of algebraic equations gives discrete pressure values evaluated at each well in each permeable layer. With the assumption of vertical equilibrium within each permeable formation, and the analytical solutions for pressure variations moving radially away from any well, the pressure field becomes known at all points in space.

Next the calculated pressures are used to update fluid flows, with the update augmented by upconing calculations around all leaky wells to determine the impact of leakage on the location of the CO₂–brine interface locally. Finally, all CO₂ plumes are updated to properly redistribute mass according to the pressure and flow fields. Once all pressures, flow rates, and CO₂ plume shapes are updated, the time step is advanced and the procedure is repeated for the next time step. We have found this algorithm to be robust and efficient, and to provide reliable computations of the critical variables in the problem. Herein, we apply the model to a specific field location to show how the model can be applied to estimate potential leakage in complex, realistic domains.

3. Site description

We have identified a field location where a large-scale CCS activity might reasonably take place in the future. The location is southwest of Edmonton, Alberta, Canada, where four large coal-fired power plants currently emit about 30 million tonnes of CO₂ per year (Mt CO₂/yr) (Michael et al., 2009c). Furthermore, one of the plant operators intends to implement at a new generation unit a commercial scale demonstration CCS project. The project, designed to capture approximately 1 Mt CO₂/yr, has received significant financial support from the Alberta provincial government

and from the Canadian federal government and is expected to be operational by 2015. The location of our study area is shown in Fig. 4. Data have been collected for site characterization in the area outlined in the figure, with the area being 50 km × 50 km. Within that area, 1146 existing oil and gas wells have been identified. The locations of these wells are shown in Fig. 4. These wells have variable characteristics, including depth of penetration and age. We have also identified the general stratigraphic sequence in the area (shown in Fig. 4), which consists of alternating permeable and impermeable layers, with the permeable layers corresponding to sandstones in the higher layers and carbonates in the lower layers. The impermeable caprock formations are shales. The characteristics of the permeable layers, including number of wells, are summarized in Table 1. Additional information can also be found in Michael et al. (2009c) and on the Alberta Geological Survey (AGS) website <http://www.ags.gov.ab.ca/>.

The average slope of the different formations across the area was determined by examination of well logs associated with the different wells, and the associated estimation of vertical locations of the different formations. In general, the slopes are less than 1%. When considered in the context of the analysis presented by Gasda et al. (2008), we conclude that the buoyant movement of the CO₂ injection plume due to caprock slope will be insignificant during the entire period of injection. As such, the assumption of horizontal formations may be seen as reasonable.

The permeable layers have associated with them a number of small-scale (core-plug) measurements of permeability. These have been aggregated into formation averages (see Michael et al., 2009c) as shown in Table 1. We use these estimates directly in our simulations. All caprock formations are assumed to be impermeable, except for possible flows along the existing wells. We have assigned an effective compressibility for the system of $c_{eff} = 4.6 \times 10^{-10} \text{ m}^2/\text{N}$. We take the domain size to be 50 km × 50 km, although we have assigned lateral fixed-pressure boundary conditions along boundaries that are typically taken to be much larger than the 50 × 50 domain of interest (see later discussion about r_{outer}), with the values along these outer boundaries held constant at the initial values, which are taken to be hydrostatic conditions within all formations. The boundary condition at the injection well is a fixed flux equal to Q_{well} . Initially, all formations are saturated with brine at hydrostatic pressure. The bottom of the deepest permeable formation – Basal Sandstone – is taken as the bottom boundary, with a no-flow condition imposed. The top-most layer is taken as a 30 m thick, 20 millidarcy permeable aquifer just above a very thick aquitard located between the depths of 30 m and 728.8 m. A no-flow condition is also imposed at the top of this top-most aquifer. We report accumulations of mass in the uppermost permeable formation as an indication of the amount of mass that would continue to move upward toward the land surface. Note that we do not include any phase change for the CO₂ as it moves upward via leakage along wells, since CO₂ is in supercritical phase in all aquifers listed in Table 4 except for the Belly River aquifer.

Each of the 1146 existing oil and gas wells within the domain is assigned a finite depth, based on well logs and records. Depending on its depth, any given well will perforate a sequence of caprock formations, and eventually end in a specific formation. We have collectively grouped all of the wells based on the deepest formation penetrated. Table 1 shows this information. We see, for example, that about 900 wells perforate the caprock of the Viking Formation, 719 perforate the caprock of the Nordegg/Banff Formation, and then there is a large drop, to 39 wells, penetrating the Nisku Formation (the large drop in the number of wells is due to the fact that the upper units are oil and gas producing, while the lower ones are not). As must be the case, the number of wells perforating the caprock formation above any given permeable formation decreases as one proceeds deeper into the vertical succession.

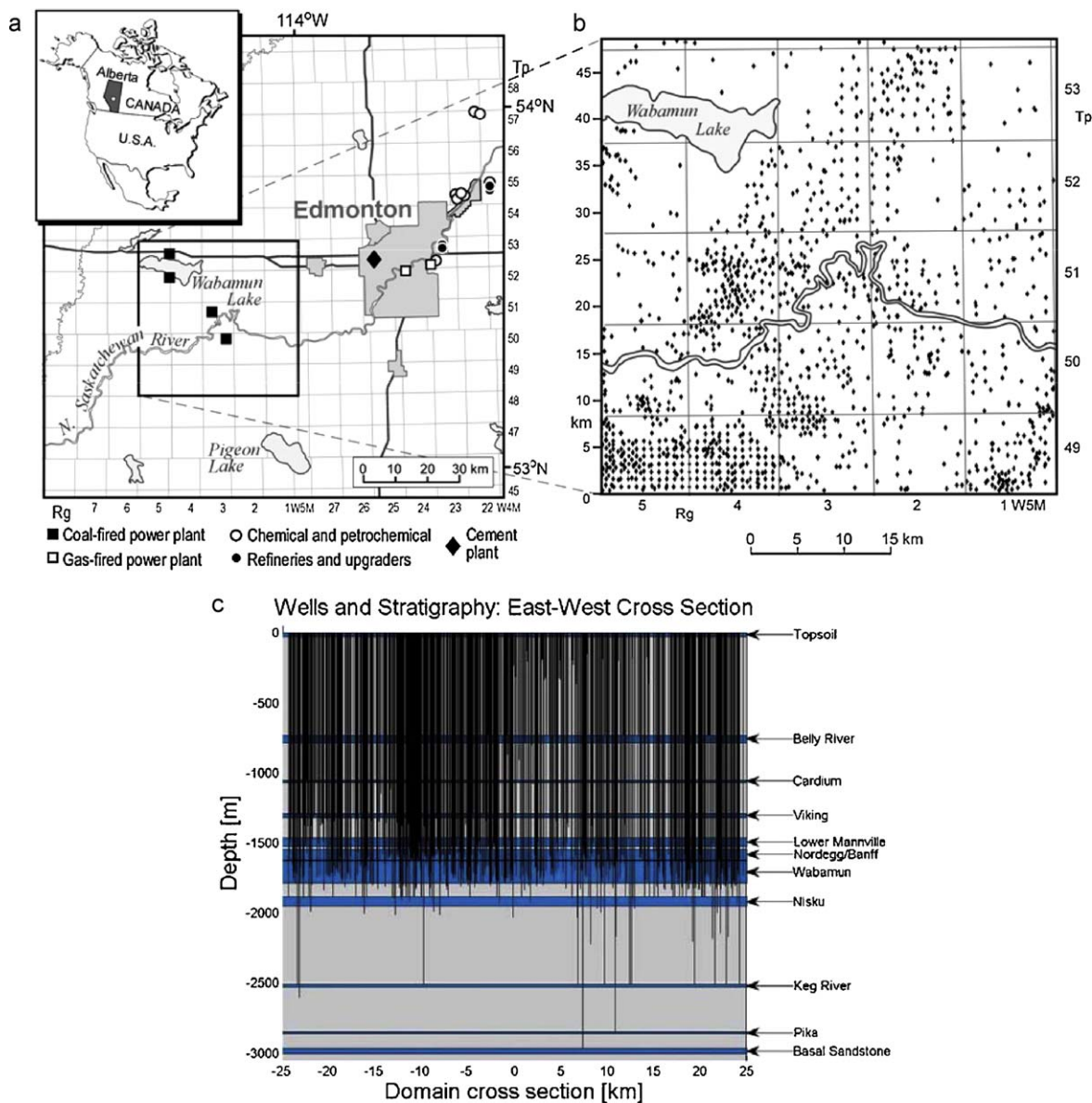


Fig. 4. Wabamun Lake area study site in Alberta, Canada, with both a top view and vertical section of all wells in the domain.

4. Computational algorithm and parameter choices

Our computational approach is based on assignment of all formation properties deterministically, using the values listed in Table 1. Because of the overwhelmingly large uncertainty associated with properties assigned to leaky wells, we take the effective

well permeabilities to be the dominant uncertainty and treat that parameter stochastically. Each well is divided into segments, with a segment defined as the section of well that crosses one caprock formation. Effective permeability values are assigned randomly to each well segment based on specified probability distributions. Because very few measurements of effective permeability along

Table 1
Characteristics of permeable layers in the study area. Shaded rows correspond to formations into which injection is simulated. Data in columns marked with * are from Michael et al. (2009c).

Aquifer name*	Top depth [m]	Thickness [m]*	Intrinsic permeability [milliDarcy]*	Porosity*	Wells ending in layer
Belly River	728.8	56	86	0.15	1146
Cardium	1051.8	15	7	0.19	1131
Viking	1287.8	30	53	0.11	878
Mannville	1461.8	65	7	0.14	874
Nordegg/Banff	1537.8	80	4	0.10	719
Wabamun	1628.8	160	4	0.12	136
Nisku	1881.8	72	170	0.12	39
Keg River	2506.8	22	3.5	0.12	11
Pika	2844.8	14	16	0.12	2
Basal Sandstone	2964.8	38	23	0.12	1

Table 2

Mapping of well score to mean effective well permeability. Data in columns marked with * from Watson and Bachu (2008).

Deep leakage potential*	Score range*	Well effective permeability mean [mD]
Low	<2	0.01–0.02
Medium	2–6	0.02–0.5
High	6–10	0.5–8
Extreme	>10	8–10,000

well segments have been reported in the literature (see the recent work of Crow et al. (2010) for one example), we are motivated to use the recent analyses of well characteristics by Watson and Bachu (2008, 2009). Watson and Bachu developed a scoring system meant to represent the likelihood that a well will leak based on “soft” information about various well characteristics such as well type, depth, time of drilling, completion and abandonment, and regulatory requirements at these times, rather than actual permeability measurements (which are not available). They developed two metrics: a Deep Leakage Potential associated with the well segments in the deeper caprock formations overlying the deepest formation reached by a given well, and a Shallow Leakage Potential associated with well segments across all shallower caprock layers. Both metrics are based on a set of attributes for each well in Alberta inclusive of the study area. For example the Deep Leakage Potential is based on: number of perforations, treatment of producing intervals, and abandonment type. We have developed a simple algorithm to map the scores identified by Watson and Bachu (2008, 2009) into a probability distribution for values of effective permeability. We do this with a direct map of score into the mean of a lognormal probability distribution with unit variance. A given score is then translated into an effective permeability by a random choice from this probability distribution. Relevant information associated with the mapping of scores into permeabilities is provided in Table 2. This method to estimate effective permeabilities along well segments provides an alternative to our earlier approach, in which we had assumed *a priori* probability distributions for effective well permeability (see, for example, Celia et al., 2006 or Kavetski et al., 2006). Those distributions were bi-modal lognormal distributions with one mode corresponding to intact cement and the other corresponding to degraded cement regions. For the current application, we have used both the scoring approach and the bi-modal distribution, although we focus on the scoring system for most of the results.

When assigning effective permeability values to segments of a particular well, we have allowed for two different choices of spatial correlations. The first assumes that all segments along a given well have permeability values that are independent and uncorrelated. As such, the permeability value for each segment is chosen independently. The second assumes that the quality of materials in a given well is uniform along the entire well, which means that the effective permeability values are completely correlated. In this case, one value of effective permeability is chosen from the probability distribution, and that value is assigned to all segments of a given well. Note that the results shown herein will compare two scenarios of simulations where permeability values assigned along a given well were either fully correlated or fully uncorrelated. For all cases, we assume no horizontal correlation so that the values assigned to one well are independent of values assigned to any neighboring wells.

For a given probability distribution and correlation structure, one thousand simulations were run, each using a different set of randomly generated effective permeability values. The outputs that we analyze include CO₂ and brine leakage after 50 years of injection, and the calculated pressure pulse in the system. All simulations use one vertical injection well, placed at the center of the domain,

Table 3

Maximum injection rates in each aquifer for different brine residual saturation scenarios. Data in columns marked with * from Bennion and Bachu (2008).

Aquifers' injection rates [Mt CO ₂ /yr]	Case 1: $S_B^{res} = 0$; $k_{rel,C} = 1$	Case 2: $S_B^{res} = 0.3$; $k_{rel,C} = 0.55^*$	Case 3: Measured S_B^{res} and $k_{rel,C}^*$
Nordegg/Banff	0.35	0.25	0.25
Nisku	17.44	12.30	5.93
Basal Sandstone	2.30	1.58	1.58

with injection taking place in only one formation for any given simulation. Injection rates are determined based on the maximum allowable injection, constrained by the pressure at the injection well not exceeding 90% of the estimated fracture pressure as per regulatory requirements in Alberta.

5. Results

We use a number of injection scenarios to demonstrate several general results. These include (1) the importance of residual brine saturation on injection rate limitations; (2) the impact of depth of injection on risk of leakage; (3) the characteristics of brine leakage and its relationship to CO₂ leakage; and (4) the critical role played by choices for the assignment of leaky well parameters. We consider injection into three of the permeable formations listed in Table 1: the Nordegg/Banff Formation, the Nisku Formation, and the Basal Sandstone Formation. These cover a characteristic range of formation behaviors, including limits on injectivity and the number of wells penetrating the respective caprock formations.

5.1. Residual brine saturation and limits on injection rates

We inject CO₂ into each of the formations based on the maximum allowable injection pressure. According to injection regulations in Alberta, the maximum bottom hole pressure should not exceed 90% of the fracture pressure of the injection formation. We use a fracture pressure gradient of 20 kPa/m, as used in Michael et al. (2009c), and consider three different values of residual brine saturation (S_B^{res}) and the associated CO₂ relative permeability ($k_{rel,C}$) within the given injection formation. Case 1 assumes S_B^{res} is equal to zero and hence $k_{rel,C}$ is equal to 1. Case 2 assumes that all permeable formations have the same properties as those of the Basal Sandstone: $S_B^{res} = 0.3$ and the associated relative permeability evaluated at this value of saturation is $k_{rel,C} = 0.55$ (taken from Fig. 3g in Bennion and Bachu, 2008). In Case 3, each formation is assigned the specific measured values for S_B^{res} and $k_{rel,C}$ when available from the measurements reported in Bennion and Bachu (2008), otherwise the formation is assigned the values from the Basal Sandstone formation. For all simulations, values of density and viscosity were set to 479 kg/m³ and 0.0395 mPa s for CO₂ and 1045 kg/m³ and 0.2535 mPa s for brine (following from Tables I and II in Nordbotten et al., 2005a). As stated previously, we do not include a drying front in the analysis, so its impact on injectivity through time is not considered.

Results for maximum injection rates for these three cases are shown in Table 3. Note that the different choices for relative permeability evaluated at residual saturation have a substantial effect on the maximum injection rate. As shown in the table, the maximum allowable injectivity in the Nordegg Formation is reduced by about 27% between Cases 1 and 2. In the Nisku Formation it is reduced by about 30% between Cases 1 and 2 and 52% between Cases 2 and 3. In the Basal Sandstone Formation the injection rate is reduced by 32% between Cases 1 and 2. Note that these reductions are significant relative to the total emissions that need to be sequestered (30 Mt/yr). While the Nisku formation can take about

17 Mt/yr when there is no reduction to the relative permeability, when the estimated value of relative permeability at residual saturation for Case 3 is used, that injection rate is reduced to about 6 Mt/yr. The Nisku has, by far, the largest injectivity of all the formations. So this reduction in injectivity means that the domain goes from one that can accept a large majority of the annual emissions to one that can accept well below 50% of those emissions, under an assumption of a single vertical injection well. Hence residual brine saturation, and the associated reduction in CO₂ relative permeability, is a critical parameter in CO₂ injection scenarios.

These reductions in injectivity also have a significant impact on the resulting CO₂ plume size and hence on the associated number of wells contacted by the CO₂. The relevant numbers are shown in Table 4. For example, even though the Nordegg Formation has more than an order of magnitude more wells penetrating its caprock, the low injectivity of the formation leads to a maximum injection rate that is almost two orders of magnitude lower than that for the Nisku Formation. This leads to a much smaller CO₂ plume, which in turn contacts very few wells in the Nordegg Formation.

While the size of the CO₂ plume is strongly influenced by the residual brine saturation through the reduced CO₂ permeability, the spatial extent of the pressure pulse is not affected significantly. This is because the pressure calculation uses a fixed value of reservoir permeability and compressibility for the system, independent of the location of the CO₂ plume, as described in Section 2.1 (Eqs. (4)–(6)). The important characteristic of the pressure pulse is that it tends to extend much further than the CO₂ plume, and therefore the zone of elevated pressure contacts many more wells than the CO₂ plume. This can be seen in Table 4. To avoid non-physical interactions with the outer boundary of the domain, we set the outer boundary (with a fixed pressure condition) at a radius of 130 km from the injection well. We note that for injection into the Nisku Formation, the maximum extent of the pressure pulse reaches 72 km after 50 years of injection. In the Nordegg Formation the extent of the pressure pulse is 11 km, and in the Basal Sandstone Formation it is about 26 km after 50 years of injection. As noted earlier, these are affected most strongly by the limited injection rates in the different formations.

5.2. Depth of injection and its impact on risk of leakage

Because the number of wells penetrating the caprock associated with a given injection formation generally decreases as a function of increasing depth, the initial assumption is that risk of leakage should decrease continuously as a function of depth. That is true, assuming the CO₂ plume size and the pressure field are the same for all formations. However, as seen in the previous set of results, the size of a single CO₂ plume is constrained by the maximum pressure at the injection well which in turn constrains the injection rate. Therefore if we consider a single injection well, a formation with more wells penetrating its caprock may or may not have a higher risk of leakage. We observe this in the following results, which we take to be based on only one injection well. In general, the overall leakage risk clearly depends on many factors, with the number of wells being only one of those factors.

To examine the effect of depth of injection on leakage of CO₂ and brine, we consider injection into both the Nordegg and the Nisku formations, and examine the overall leakage that develops in the system. We do this by running one thousand simulations for injection into each of the two formations identified above, with a given set of stochastic parameters (which are the effective permeabilities of the well segments) to define the system, and we examine the resulting histogram of leakage amounts for both CO₂ and brine. In Figs. 5 and 6 we plot the total amounts of CO₂ and brine that leak from the injection formation, assuming a single injection well that injects at the maximum permissible rate and using the data from

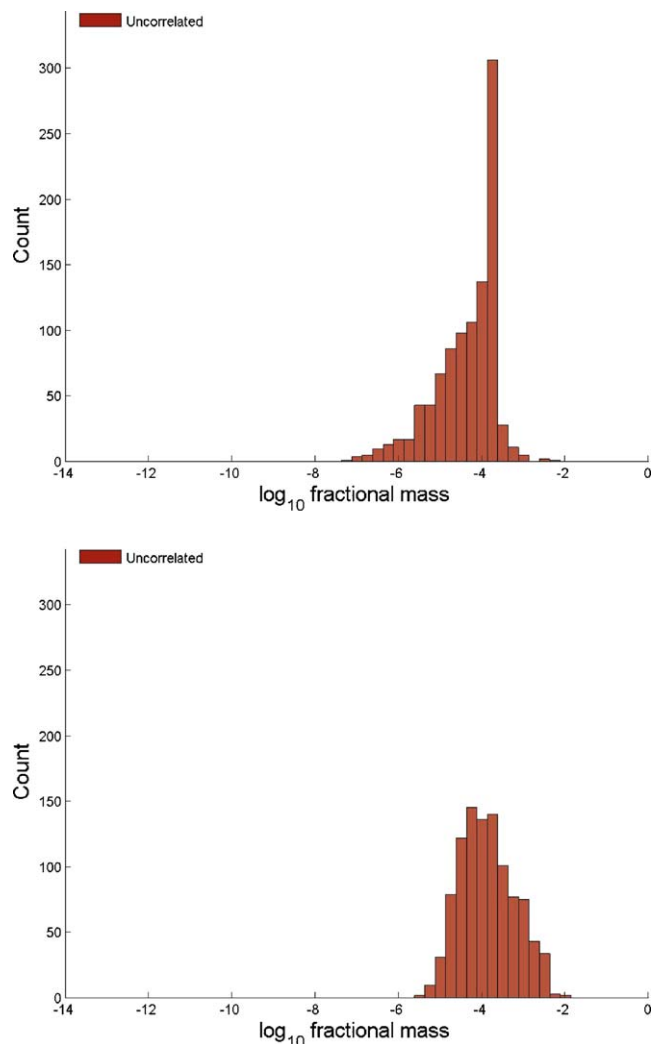


Fig. 5. Total CO₂ fractional mass leakage (Total mass leaked out of the injection formation/Total mass injected) for the Nordegg (top) and Nisku (bottom) formations, with the scoring system used for well permeabilities. Permeability values are uncorrelated. Residual saturations and relative permeabilities correspond to Case 2 ($S_{res} = 0.3$; $k_{rel} = 0.55$).

the middle column of Tables 3 and 4 (that is, residual saturation of brine of 30% and relative permeability to CO₂ being 0.55). We represent the total amount of CO₂ that leaks out of the injection formation by the fraction of the total injected mass—this is shown on the horizontal axis in Fig. 5. We do this for injection into both the Nordegg and Nisku formations. We see that the limited injectivity, and associated small number of leaky wells contacted by the CO₂ plume, especially in the Nordegg Formation, give leakage amounts for injection into the Nordegg Formation that are about an order of magnitude lower than those for injection into the Nisku Formation, despite the much larger number of wells overall in the Nordegg formation. We also observe that, for the permeabilities based on the well scores of Watson and Bachu (2008, 2009) (see Table 2), for all cases the amounts for CO₂ leaked does not exceed 1% and for almost all cases it does not exceed 0.1%, for both formations. When we examine similar results for the brine leakage, we see that the larger number of wells impacted by the pressure pulse leads to the largest brine leakage cases occurring for injection into the Nordegg Formation, followed by the Nisku Formation. The brine leakage results, presented as a fraction of the volume of injected CO₂, can be seen in Fig. 6 for the scenarios of injection into the Nordegg and Nisku formations.

Table 4Number of wells contacted by CO₂ plume and pressure pulse. Data in columns marked with * from Bennion and Bachu (2008).

	Number of wells reaching this layer	Number of wells contacted by the CO ₂ plume			Number of wells contacted by the pressure pulse
		$S_B^{res} = 0; k_{rel,C} = 1$	$S_B^{res} = 0.3; k_{rel,C} = 0.55^*$	Measured S_B^{res} and $k_{rel,C}^*$	
Nordegg/Banff	719	4	1	1	140
Nisku	39	21	17	2	39
Basal	1	1	0	0	1

While the issue of leakage risk versus depth of injection is obviously related to the number of wells that penetrate the caprock of a given formation, the injectivity of a single vertical well also plays a central role. As these calculations imply, the design of injection wells will play an important part because injection well locations and numbers will dictate what part of the domain is contacted by the CO₂ plume and pressure buildup. These decisions, in turn, depend on the injectivity of the formation, which depends on the permeability, thickness, depth, initial pressure, and residual brine saturation and the associated CO₂ relative permeability. We have chosen to use only one injection well for the purpose of consistency across the different simulations, but this clearly brings the

size of the CO₂ plume into consideration and with it many other factors in addition to simply the number of wells penetrating a given formation.

5.3. Characteristics of CO₂ leakage and of brine leakage

As we have already observed, the larger spatial footprint associated with the pressure pulse, as compared to the footprint of the CO₂ plume, tends to drive brine leakage through many more wells than those wells contacts by the injected CO₂. This means that brine leakage tends to occur over a much larger sample of the wells penetrating a formation, and therefore the brine leakage tends to reflect the number of wells in the formation, even for a single injection well. While this can be a general expectation, it is instructive to examine the leakage patterns of CO₂ and brine in somewhat more detail to observe characteristic spatial patterns in the vertical direction. For example, while Figs. 5 and 6 show the total amount of CO₂ and brine that leaves the injection formation, Figs. 7 and 8 show the amounts of CO₂ and brine that leak into the top-most formation in the domain. We see that most of the CO₂ that leaks does not reach the shallow subsurface zones, and even less of the brine reaches the shallow zones. This highlights the potentially important role played by intermediate permeable formations between the injection formation and the shallow subsurface (often referred to as secondary barriers to leakage; see Nordbotten et al., 2004; Oldenburg, 2008). More of the CO₂ makes it to the shallow zones because of the buoyant drive that combines with the pressure drive associated with injection. The brine is driven only by the imposed pressure gradients, and lacks the additional buoyant drive. Therefore there is a weaker vertically upward drive, and this is reflected in Figs. 7 and 8. The two dominant characteristics of the brine versus CO₂ leakage are the presence (or absence) of buoyant flow components, and the much larger spatial footprint of the pressure pulse as compared to the CO₂ plume. These should be taken into account when making any analysis of leakage potential and associated suitability of a given site or formation.

5.4. Dependence on stochastic parameters

Clearly, all of the results generated using our model of leakage depend on the assignment of leakage properties for the existing wells, which means the assignment of the values of effective permeability along each well segment. When using the scoring system of Watson and Bachu (2008, 2009), the mapping between well scores and effective permeabilities is the crucial step. Our approach for the current work is summarized in Table 2. Until we develop a set of data points with which to populate this kind of transformation (see, for example, Crow et al., 2010), these mappings will remain hypothetical, constrained only by expert opinion and simple estimates associated with micro-annular flows. In lieu of a scoring system, we have used a bi-modal lognormal distribution to describe the effective permeabilities, with one mode corresponding to 'good cement' and a second mode corresponding to 'bad cement'. We characterize this bi-modal distribution by the mean values of the two modes, as done, for example, in Celia et al. (2006) and Kavetski et al. (2006). Celia et al. (2009) compared simula-

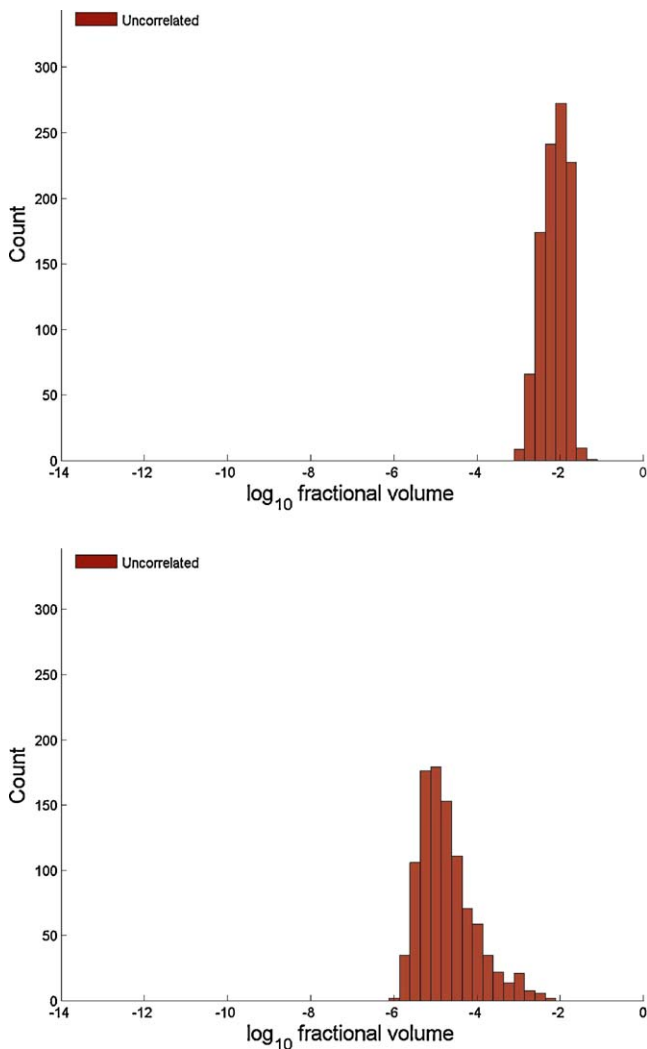


Fig. 6. Total brine fractional volume leakage (Total brine volume leaked out of the injection formation/Total CO₂ volume injected) for the Nordegg (top) and Nisku (bottom) formations with the scoring system used for well permeabilities. Permeability values are uncorrelated. Residual saturations and relative permeabilities correspond to Case 2 ($S_{res} = 0.3; k_{rel} = 0.55$).

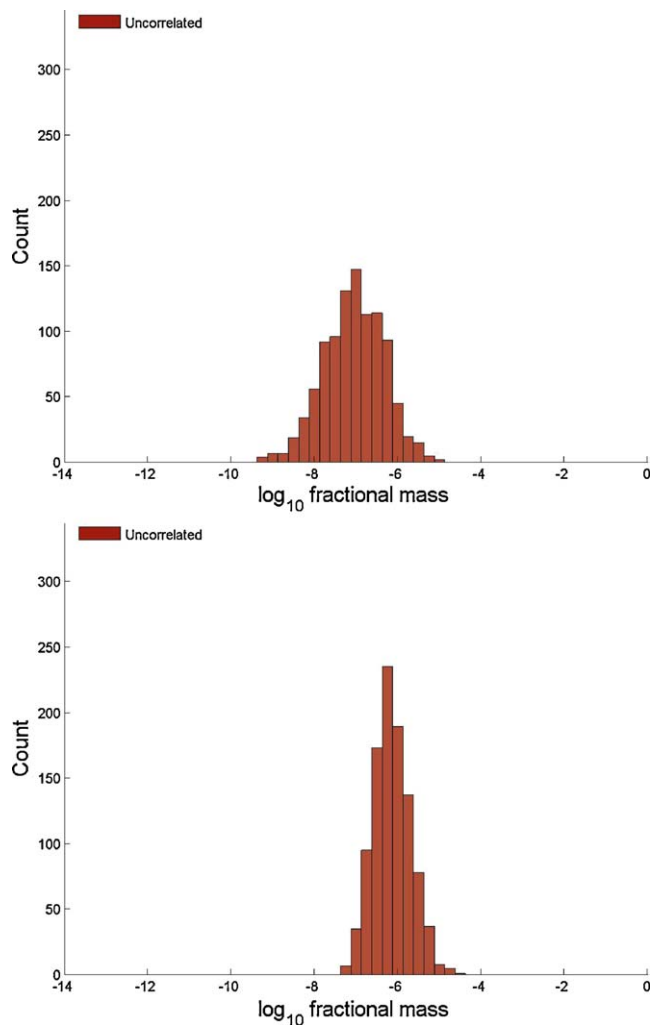


Fig. 7. Shallow zone CO₂ fractional mass leakage (Total mass leaked into the shallow zone/Total mass injected in the injection formation) for the Nordegg (top) and Nisku (bottom) formations with the scoring system used for well permeabilities. Permeability values are uncorrelated. Residual saturations and relative permeabilities correspond to Case 2 ($S_{res} = 0.3$; $k_{rel} = 0.55$).

tions using these two different approaches for assignment of well permeabilities. Among other things, their results showed that the distribution of well permeability values affects the shapes of the resulting leakage histograms. In general, the overall magnitudes of leakage are strongly controlled by the actual values assigned in the mappings as well as the means for the bi-modal distribution. These are the critical parameters and our overall lack of knowledge about these parameters argues strongly for the need for a comprehensive, systematic experimental program to identify these values.

In addition to the actual distributions used, another important consideration is the degree of correlation along a given well and among adjacent wells. For example, along a given well, each well segment might be assigned values of permeability that are independent of all other values assigned to other sections along that well. This means there would be no correlation among those values. Conversely, one might argue that a bad cement job means that all values along a given well should have similar values of permeability. If a well is assigned the same permeability values to all segments along its vertical extent, then those values will be perfectly correlated. Any degree of correlation between these two limits is possible. To examine the impact of correlation, we have conducted numerical experiments for the case of fully uncorrelated

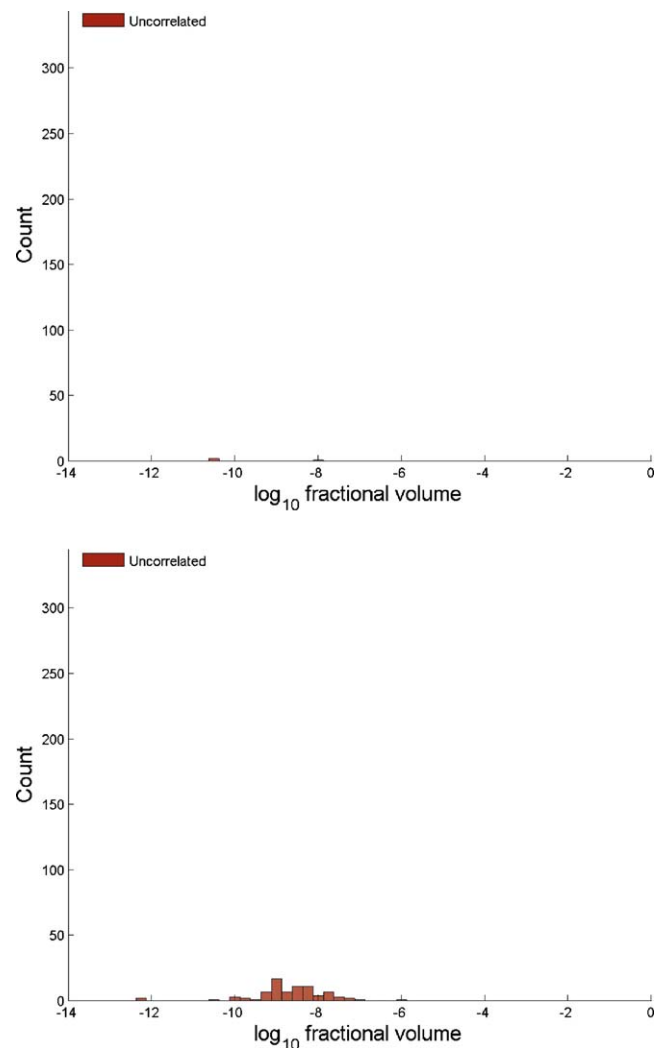


Fig. 8. Shallow zone brine fractional volume leakage (Total brine volume leaked into the shallow zone/Total CO₂ volume injected in the injection formation) for the Nordegg (top) and Nisku (bottom) formations with the scoring system used for well permeabilities. Permeability values are uncorrelated. Residual saturations and relative permeabilities correspond to Case 2 ($S_{res} = 0.3$; $k_{rel} = 0.55$).

permeability values and fully correlated values. For each case, we have assigned values to the wells as described previously, but now either all segments along the well are assigned the same value, or each segment is generated independently (note that all previous results have assumed an uncorrelated data structure for the well permeabilities).

Fig. 9 shows results for the bi-modal distribution, using fully correlated and fully uncorrelated values for well permeabilities where the two mean values for the bi-modal distribution were set to 0.1 milliDarcy and 1 Darcy, respectively, and 50% of the wells, chosen randomly, were assumed to have 'good cement' with the remaining 50% having 'bad cement'. Each mode was assigned a unit variance in log space. We again use the Nordegg and Nisku formations with the residual brine saturation of 30% and CO₂ relative permeability of 0.55. We see that the correlation structure has a major effect on the resulting CO₂ leakage amounts. The correlated structure allows much more CO₂ to leak toward the surface, in these cases increasing the fraction of CO₂ leaked by 4–5 orders of magnitude. Similar results are seen for permeabilities based on the scoring system, although for the parameters in Table 2 the differences are only one to two orders of magnitude. The corresponding results are shown in Fig. 10.

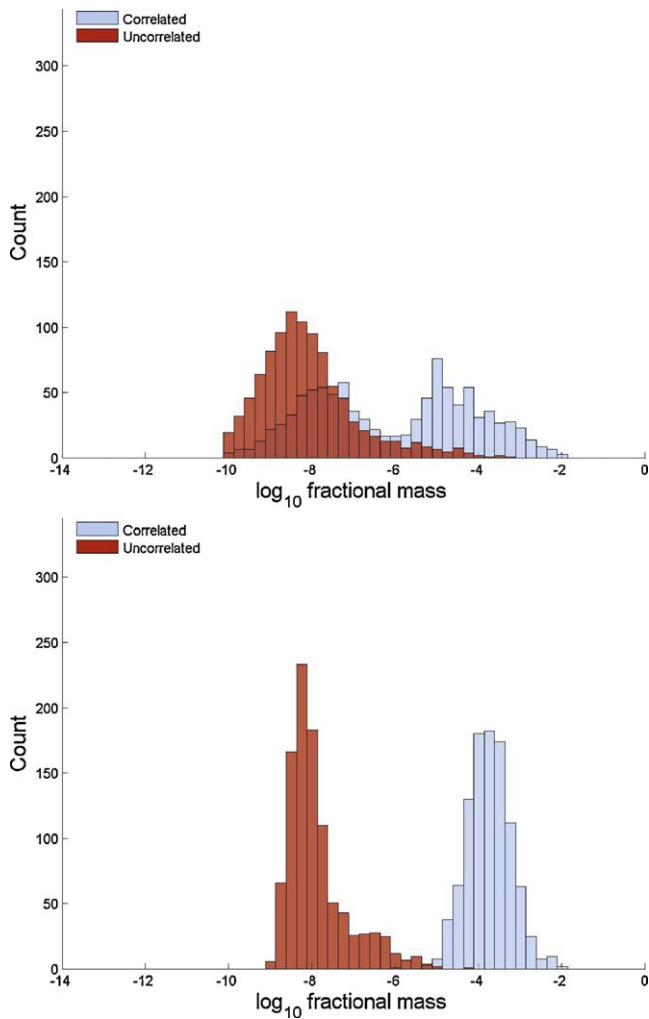


Fig. 9. Shallow zone CO₂ fractional mass leakage for the Nordeg (top) and Nisku (bottom) formations for Case 2 comparing the bimodal 50% weight distribution fully correlated (blue) and uncorrelated (red). (For interpretation of the references to color in this figure legend, the reader is referred to the web version of the article.)

These results are consistent with our understanding of the system. In the one-dimensional flow system corresponding to a leaky well, the effective permeability is controlled by the segment with the lowest permeability. Thus, when permeabilities are fully uncorrelated, the only way to have a large permeability along the entire length of a well is for all of the segments to have high values. When each value is chosen independently from a given probability distribution, the probability of all values being large is relatively low. Hence the probability of a large leakage value is also low, resulting in the much lower estimates for leakage to shallow zones in systems where the well permeabilities are uncorrelated. Conversely, when all of the values are correlated, once a large permeability is assigned, it persists along the entire well, leading to substantially larger leakage rates into shallow zones of the subsurface. This is clearly seen in the results, and points to another important set of data that must be determined to properly characterize well leakage.

The fact that leakage results using the bi-modal distribution show much larger impact of correlation, as compared to the scoring system, is also consistent with the characteristics of the two different approaches. While the bi-modal approach is fully random, such that each permeability value is chosen from the entire span of the bi-modal distribution, the scoring system has constrained randomness through the assignment of the score. Once a well is given

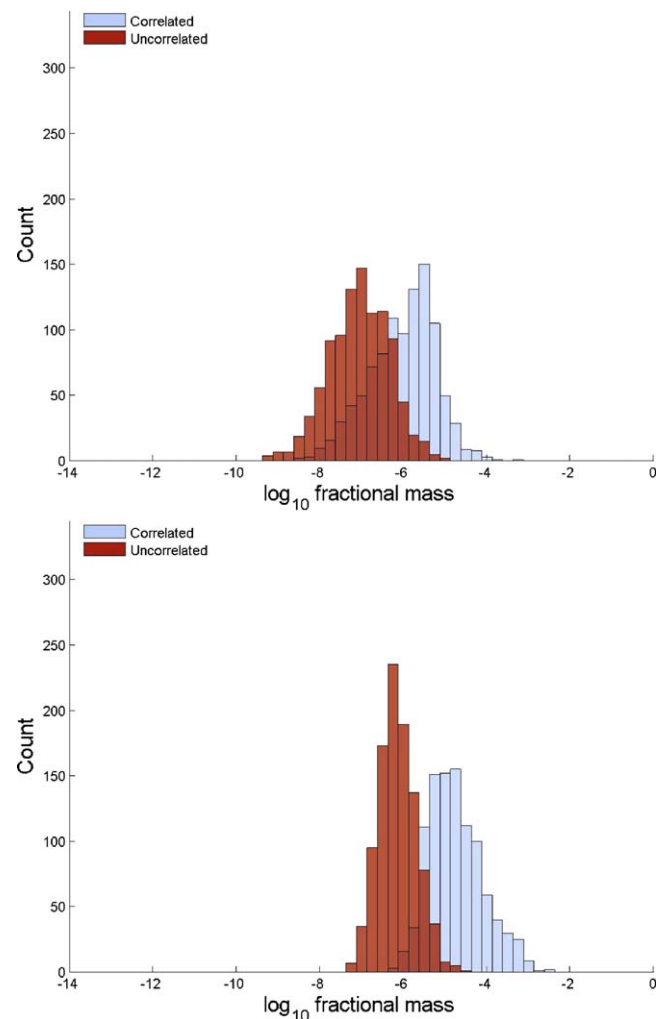


Fig. 10. Shallow zone CO₂ fractional mass leakage for the Nordeg (top) and Nisku (bottom) formations for Case 2 comparing the scoring system distribution fully correlated (blue) and uncorrelated (red). (For interpretation of the references to color in this figure legend, the reader is referred to the web version of the article.)

a score, it is then immediately given a corresponding mean permeability value, and then the probability distribution from which the permeability value is assigned is a lognormal distribution that has the assigned mean and a unit variance. This gives a significantly diminished range of values from which permeability values are assigned. This is consistent with the idea that some amount of 'soft' information is being used to constrain the randomness of the problem, and therefore should result in replacement of some of the randomness with a deterministic component. That is exactly what we see in the computational results.

Finally, we point out that after 50 years of injection, in all cases presented herein as well as a range of other cases we have run, leakage of CO₂ into the shallowest formation almost never exceeds one percent of the mass of injected CO₂, and is usually less than 0.1%. A few scenarios involving large fractions of leaky wells and injection into the Nordeg and Nisku formations can result in leakage slightly larger than one percent, while for injection into the Basal Sandstone Formation, leakage is estimated to be always less than 0.01% of the injected mass after 50 years of injection. We stress that our results obviously depend on the permeability values assigned to leaky wells, as well as our injection strategy, but over the permeability distributions we have considered leakage appears to range from modest to insignificant. With our simple injection strategy – a single vertical injection well in the center of the domain – injec-

tivity limitations become significant and could be more important than leakage considerations. More complex injection scenarios, involving multiple wells and including horizontal wells, will be considered in future work and are expected to increase the injectivity associated with these formations, with a concomitant increase in estimated leakage due to increased numbers of potentially leaky wells contacted by the plumes. The Nisku Formation, with its much higher injectivity, should be considered as the best formation for injecting captured CO₂. The Basal Sandstone Formation is the next-best choice, although its injectivity is significantly lower than that of the Nisku Formation. Finally, despite the relatively small number of potentially leaky wells contacted by the CO₂ in the Nordegg Formation, thereby leading to relatively little leakage, this formation is not very useful because its injectivity is much too low.

6. Conclusions

The semi-analytical model for CO₂ and brine migration and leakage provides a flexible and very efficient computational framework to study many aspects of the system response to CO₂ injection into deep saline aquifers. This particular model can accommodate very large numbers of potentially leaky wells (many thousands) and many alternating layers of aquifers and caprock formations. Many potential injection sites in North America are likely to have tens to hundreds, and possibly more, of existing oil and gas wells within the radius of influence of a CO₂ injection operation, and this modeling framework allows these systems to be analyzed quantitatively. Because the semi-analytical modeling framework can simulate the movement and leakage of CO₂ and brine over a typical injection period of 50 years using only a few minutes of computing time on a standard single-processor personal computer, we can explore many aspects of the system in a stochastic, or probabilistic, framework.

We have used a specific site in Alberta, Canada, in the Wabamun Lake area, to explore some of the characteristics of the system response to realistic injection scenarios. Each permeable layer in the stratigraphic sequence was assigned parameter values including porosity, permeability, thickness, residual brine saturation, and CO₂ relative permeability evaluated at the residual brine saturation, based on actual field and laboratory data. Fixed (average) values of porosity and permeability were assigned to each formation, based on measured values, and several different values of residual saturation and relative permeability were considered. As the results in Section 5 indicate, the system response involves a complex interplay among formation properties, fluid properties, and properties of the leaky wells. An important limitation on injection rates in formations like those around Lake Wabamun is the maximum pressure at the injection well, which in turn depends critically on residual saturation of the displaced brine and the associated relative permeability to the CO₂ in the region containing residual brine. Use of measured values of residual brine saturations and associated CO₂ relative permeability can reduce injection rates by up to 70%. While the measured values were from a single core plug experiment, and questions about upscaling and the appropriate large-scale effective relative permeability remain to be answered, these results indicate quite clearly that careful design of injection well location and orientation will be very important in the overall system design. While we do not address well design and well placement herein, it is a topic that can be studied with the computational modeling approach presented herein.

For all of the injection scenarios considered, the CO₂ plume was significantly smaller than the areal extent of the pressure pulse. This has implication for well design, where close spacing may be preferred to maximize CO₂ coverage within the domain but is limited due to pressure interference from adjacent wells. It also has

important implications for leakage behavior. Because the pressure pulse tends to spread much farther than the CO₂ plume, brine leakage is observed along many more leaky wells as compared to wells with CO₂ leakage. The signature of brine leakage in these layered sedimentary successions tends to differ from the CO₂ leakage due to the significant buoyant drive that contributes to upward movement of CO₂ in leaky wells but is absent from the brine leakage. Brine will leak both upward and downward, while CO₂ leaks primarily upward. Carbon dioxide also tends to migrate upward over much longer distances, being driven strongly by buoyancy, than does the leaking brine, which is driven only by the pressure increase. Therefore, more CO₂ migrates into shallow subsurface zones as compared to brine leakage, although both tend to exhibit patterns of leakage into intervening permeable layers while flowing along leaky wells, as illustrated in Fig. 3.

The lack of data for hydraulic properties of old wells requires a stochastic approach for leakage analysis, where the dominant uncertainty is in the properties of leaky wells. We have used several different methods to characterize the randomness of the effective permeability of the well materials and surrounding damage zone in the rock. When no information is available to constrain the parameters, then a purely random method is used with a given probability distribution used to assign well properties randomly. When qualitative information about the wells is available, a systematic evaluation of those data, like that used by Watson and Bachu (2008, 2009), may be used to constrain the randomness. In those cases, the well properties have a mixed deterministic-stochastic nature through constraints on the probability distributions used to define the effective well permeabilities. These and other stochastic approaches fit naturally into the computational model we have developed.

Independent of the specific probability distributions used to define the well properties, another critical choice in the parameter description involves spatial correlation. Along a given well, a single effective permeability may be assigned to the entire length of the well, or each well segment along the vertical direction may be assigned a different value of well permeability. The first case, involving only a single value for a given well, may be seen as using values for each segment that are completely correlated and therefore identical. In the second case, if all segments along a given well are assigned permeability values that are independent of one another, then the values may be seen as being completely uncorrelated. The correlation structure assigned along a given well plays an important role in the amount and nature of the resulting leakage. Additional spatial correlation among neighboring wells may also be assigned, although we have not explored this kind of correlation to date.

While the semi-analytical model is able to provide many insights into the overall system behavior, it is clearly limited in its scope by the restrictive assumptions on which it is based. Our current work is moving toward hybrid models that can provide numerical solutions in regions where the restrictive assumptions are not applicable, while continuing to use analytical solutions in regions where they are appropriate. We are also working with other groups to try to develop the beginnings of a data base for appropriate hydraulic properties for old – and potentially leaky – oil and gas wells. We believe these additions in both model capabilities and in data collection will allow for reductions in uncertainties and associated increases in confidence as large-scale field sites are studied for possible injection of captured CO₂.

Acknowledgements

This work was supported in part by the National Science Foundation under Grant EAR-0934722; the Environmental Protection

Agency under Cooperative Agreement RD-83438501; the Department of Energy under Award No. DE-FE0001161, CFDA No. 81,089; and the Carbon Mitigation Initiative at Princeton University.

References

- Alberta Geological Survey website <http://www.ags.gov.ab.ca/>.
- Bachu, S., Celia, M.A., 2009. Assessing the potential for CO₂ leakage, particularly through wells, from geological storage sites. In: McPherson, B.J., Sundquist, E. (Eds.), *The Science of CO₂ Storage*. Geophysical Monograph Series GM148. American Geophysical Union, Washington, DC, USA.
- Bennion, D.B., Bachu, S., 2008. Drainage and imbibition relative permeability relationships for supercritical CO₂/brine and H₂S/brine systems in intergranular sandstone, carbonate, shale and anhydrite rocks. *SPE Reservoir Eval. Eng.* 11 (3), 487–496. DOI: 19.2118/99326PA.
- Birkholzer, J.T., Zhou, Q., Tsang, C.-F., 2009. Large-scale impact of CO₂ storage in deep saline aquifers: a sensitivity study on the pressure response in stratified systems. *Int. J. Greenhouse Gas Control* 3 (2), 181–194.
- Celia, M.A., Bachu, S., Nordbotten, J.M., Kavetski, D., Gasda, S.E., CD ROM, Elsevier 2006. A risk assessment modeling tool to quantify leakage potential through wells in mature sedimentary basins. In: Gale, J., Rokke, N., Zweigel, P., Svenson, H. (Eds.), *Proceedings of the 8th International Conference on Greenhouse Gas Control Technologies*. Trondheim, Norway, June 19–22.
- Celia, M.A., Nordbotten, J.M., 2010. How simple can we make models for CO₂ injection, migration, and leakage? In: *Proceedings of the 10th International Conference on Greenhouse Gas Control Technologies*, Amsterdam, September, p. 2010.
- Celia, M.A., Nordbotten, J.M., 2009. Practical modeling approaches for geological storage of carbon dioxide. *Ground Water* 47 (5), 627–638.
- Celia, M.A., Nordbotten, J.M., Bachu, S., Dobossy, M., Court, B., 2009. Risk of leakage versus depth of injection in geological storage. In: *Proceedings of the 9th International Conference on Greenhouse Gas Control Technologies*, Washington, DC, November 16–20, 2008, Elsevier, *Energy Procedia* 1 (1), pp. 2573–2580.
- Crow, W., Carey, J.W., Gasda, S., Williams, B., Celia, M.A., 2010. Wellbore integrity analysis of a natural CO₂ producer. *Int. J. Greenhouse Gas Control* 4, 186–197.
- Dentz, M., Tartakovsky, D.M., 2009. Abrupt-interface solution for carbon dioxide injection into porous media. *Transport Porous Media* 79 (1), 15–27.
- Gasda, S.E., Bachu, S., Celia, M.A., 2004. Spatial characterization of the location of potentially leaky wells penetrating a deep saline aquifer in a mature sedimentary basin. *Environ. Geol.* 46 (6–7), 707–720, doi:10.1007/s00254-004-1073-5.
- Gasda, S.E., Nordbotten, J.M., Celia, M.A., 2008. Upslope plume migration and implications for geological CO₂ sequestration in deep saline aquifers. *IES J Part A: Civil Struct. Eng.* 1 (1), 2–16.
- Grimstad, A.-A., Georgescu, S., Lindeberg, E., Vuillaume, J.-F., 2009. Modelling and simulation of mechanisms for leakage of CO₂ from geological storage. *Energy Procedia* 1 (1), 2511–2518.
- Hesse, M.A., Tchepeli, H.A., Cantwell, B.J., Orr Jr., F.M., 2007. Gravity currents in horizontal porous layers: transition from early to late self-similarity. *J. Fluid Mech.* 577, 363–383.
- Hesse, M.A., Orr Jr., F.M., Tchepeli, H.A., 2008. Gravity currents with residual trapping. *J. Fluid Mech.* 611, 35–60.
- Hunt, B., 1985. Flow to a well in a multiaquifer system. *Water Resour. Res.* 21 (11), 1637–1641.
- IEA (International Energy Agency), 2004. *Prospects for CO₂ Capture and Storage*. IEA/OECD, Paris, France.
- IEA (International Energy Agency), 2008a. *Energy Technology Perspectives: Scenarios and Strategies to 2050*. IEA/OECD, Paris, France.
- IEA (International Energy Agency), 2008b. *CO₂ Capture and Storage: A Key Abatement Option*. IEA/OECD, Paris, France.
- Intergovernmental Panel on Climate Change (IPCC), 2005. In: Metz, B., Davidson, O., de Coninck, H., Loos, M., Mayer, L. (Eds.), *Special Report on Carbon Dioxide Capture and Storage*. Cambridge University Press, Cambridge, UK/New York, NY, USA.
- Kavetski, D., Nordbotten, J.M., Celia, M.A., 2006. Analysis of potential CO₂ leakage through abandoned wells using a semi-analytical model. In: Binning, P.J., Engesgaard, P., Dahle, H., Pinder, G., Gray, W. (Eds.), *Proceedings of the XVI International Conference on Computational Methods in Water Resources*. Copenhagen, Denmark, June 2006 (accessed 19.05.09) <http://proceedings.cmw-r-xvi.org>.
- Kopp, A., Class, H., Helmig, R., 2009. Investigations on CO₂ storage capacity in saline aquifers. Part 1. Dimensional analysis of flow processes and reservoir characteristics. *Int. J. Greenhouse Gas Control* 3 (3), 263–276.
- Mathias, S.A., Hardisty, P.E., Trudell, M.R., Zimmerman, R.W., 2009a. Approximate solutions for pressure buildup during CO₂ injection in brine aquifers. *Transport Porous Media* 79 (2), 265–284.
- Mathias, S.A., Hardisty, P.E., Trudell, M.R., Zimmerman, R.W., 2009b. Screening and selection of sites for CO₂ sequestration based on pressure buildup. *Int. J. Greenhouse Gas Control* 3 (5), 577–585.
- McKinsey and Company, 2007. *Reducing U.S. Greenhouse Gas Emissions: How Much and at What Cost?* U.S. Greenhouse Gas Abatement Mapping Initiative, Executive Report.
- Michael, K., Arnot, M., Cook, P., Ennis-King, J., Funnell, R., Kaldi, J., Kirste, D., Paterson, L., 2009a. CO₂ storage in saline aquifers I—current state of scientific knowledge. *Energy Procedia* 1 (1), 3197–3204.
- Michael, K., Allinson, G., Golab, A., Sharma, S., Shulakova, V., 2009b. CO₂ storage in saline aquifers II—experience from existing storage operations. *Energy Procedia* 1 (1), 1973–1980.
- Michael, K., Stefan Bachu, B.E., Buschkuhle, K.H., Talman, S., 2009c. Comprehensive characterization of a potential site for CO₂ geological storage in Central Alberta, Canada. In: Grobe, M., Pashin, J., Dodge, R. (Eds.), *Carbon Dioxide Sequestration in Geological Media—State of the Art, AAPG Studies in Geology*, vol. 59, pp. 227–240.
- MIT (Massachusetts Institute of Technology), 2007. *The Future of Coal: Options for a Carbon-constrained World*. The Massachusetts Institute of Technology, Cambridge, MA, USA.
- Nordbotten, J.M., Celia, M.A., Bachu, S., 2004. Analytical solutions for leakage rates through abandoned wells. *Water Resour. Res.* 40 (4), W04204.
- Nordbotten, J.M., Celia, M.A., Bachu, S., 2005a. Injection and storage of CO₂ in deep saline aquifers: analytical solution for CO₂ plume evolution during injection. *Transport Porous Media* 58 (3), 339–360.
- Nordbotten, J.M., Celia, M.A., Bachu, S., Dahle, H.K., 2005b. Semianalytical solution for CO₂ leakage through an abandoned well. *Environ. Sci. Technol.* 39 (2), 602–611.
- Nordbotten, J.M., Celia, M.A., 2006a. Similarity solutions for fluid injection into confined aquifers. *J. Fluid Mech.* 561, 307–327.
- Nordbotten, J.M., Celia, M.A., 2006b. An improved analytical solution for interface upconing around a well. *Water Resour. Res.* 42 (8), W08433.
- Nordbotten, J.M., Kavetski, D., Celia, M.A., Bachu, S., 2009. Model for CO₂ leakage including multiple geological layers and multiple leaky wells. *Environ. Sci. Technol.* 43 (3), 743–749.
- Oldenburg, C.M., 2008. Screening and ranking framework for geologic CO₂ storage site selection on the basis of health, safety, and environmental risk. *Environ. Geol.* 54 (8), 1687–1694.
- Pacala, S., Socolow, R.H., 2004. Stabilization wedges: solving the climate problem for the next 50 years with current technologies. *Science* 305 (5686), 968–972.
- Pawar, R.J., Watson, T.L., Gable, C.W., 2009. Numerical simulation of CO₂ leakage through abandoned wells: model for an abandoned site with observed gas migration in Alberta, Canada. *Energy Procedia* 1 (1), 3625–3632.
- Pruess, K., 2009. Formation dry-out from CO₂ injection into saline aquifers: 2. Analytical model for salt precipitation. *Water Resour. Res.* 45, W03403.
- Pruess, K., Muller, N., 2009. Formation dry-out from CO₂ injection into saline aquifers: 1. Effects of solids precipitation and their mitigation. *Water Resour. Res.* 45, W03402.
- Schnaar, G., Digiulio, D.C., 2009. Computational modeling of the geologic sequestration of carbon dioxide. *Vadose Zone J.* 8 (2), 389–403.
- Sheppard, M.C., Socolow, R.H., 2007. Sustaining fossil fuel use in a carbon-constrained world by rapid commercialization of carbon capture and sequestration. *AIChE J.* 53 (12), 3022–3028.
- Stauffer, P.H., Viswanathan, H.S., Pawar, R.J., Guthrie, G.D., 2009. A system model for geologic sequestration of carbon dioxide. *Environ. Sci. Technol.* 43 (3), 565–570.
- Szulczewski, M., Juanes, R., 2009. A simple but rigorous model for calculating CO₂ storage capacity in deep saline aquifers at the basin scale. *Energy Procedia* 1 (1), 3307–3314.
- Watson, T.L., Bachu, S., 2008. Identification of wells with high CO₂-leakage potential in mature oil fields developed for CO₂-enhanced oil recovery. In: *Paper SPE 11294, SPE Improved Oil Recovery Symposium*, Tulsa, OK, USA, 19–23 April.
- Watson, T.L., Bachu, S., 2009. Evaluation of the potential for gas and CO₂ leakage along wellbores. *SPE Drilling Completion* 24 (March (1)), 115–126.
- Zhou, Q., Birkholzer, J.T., Tsang, C.-F., Rutqvist, J., 2008. A method for quick assessment of CO₂ storage capacity in closed and semi-closed saline formations. *Int. J. Greenhouse Gas Control* 2 (4), 626–639.